

Near instantaneous $O(1)$ Analog Solver Circuit for Linear Symmetric Positive-Definite Systems

Osama Abdelaleim, Arun Prakash, Ayhan Irfanoglu, Veljko Milutinovic

Abstract—Accelerating the solution of linear systems of equations is critical due to their central role in numerous applications, such as scientific simulations, data analytics, and machine learning. This paper presents a general-purpose analog direct solver circuit designed to accelerate the solution of positive definite symmetric linear systems of equations. The proposed design leverages non-inverting operational amplifier configurations to create a negative resistance circuit, effectively modeling any symmetric system. The paper details the principles behind the design, optimizations of the system architecture, and numerical results that demonstrate the robustness of the design. The findings reveal that the proposed system solves diagonally dominant symmetric matrices with $O(1)$ complexity, achieving the theoretical maximum speed as the circuit relies solely on resistors. For non-diagonally dominant symmetric positive-definite systems, the solution speed depends on matrix properties such as eigenvalues and the maximum off-diagonal term, but remains independent of matrix size.

Index Terms—analog computing, linear algebra, resistive networks

I. INTRODUCTION

SOLVING systems of linear equations are fundamental for addressing real-world challenges across various domains, especially in the era of big data where the volume and complexity of datasets continue to grow exponentially. Although powerful, traditional digital computing approaches are encountering limitations in parallelization and scalability, particularly as Moore’s Law is close to reaching its asymptotic plateau. Thus, accelerating the solution of linear systems of equations can be immensely impactful for applications where the ability to process vast amounts of data efficiently is paramount including scientific simulations, data analytics, machine learning and several others.

A. Existing Paradigms for Solving Large Systems of Equations

For decades, the primary engine for tackling these problems has been digital computing. Classical direct factorization methods, such as Gaussian elimination, LU decomposition, and Cholesky factorization, offer exact solutions but typically exhibit a computational complexity of $O(n^3)$, where n is the number of unknowns [1]. Iterative methods, including Jacobi, Gauss-Seidel, Successive Over-Relaxation (SOR), and Conjugate Gradient (CG), offer alternatives, particularly for

large, sparse systems [2]. While often exhibiting lower complexity $O(n^2)$ per iteration, their convergence rate depends heavily on matrix properties such as condition number [2]. As system size (n) explodes in modern applications, digital solvers, both direct and iterative, face significant bottlenecks. Executed on traditional von Neumann architectures, they have substantial time and energy overheads associated with data movement between memory and processing units, pushing power consumption and execution time to prohibitive levels [3]. This challenge motivates the exploration of fundamentally different computing paradigms such as quantum computing and analog computing.

With quantum computing, algorithms like the Harrow-Hassidim-Lloyd (HHL) algorithm theoretically promise an exponential speedup for solving certain linear systems, potentially achieving complexity of $\log(n)$ under specific conditions on the system matrix A and the desired output precision [4]. Although its long-term promise holds, quantum computing faces challenges such as qubit coherence times and error rates. Thus, it is currently not a viable option for large-scale problems [5], [6].

An alternative gaining significant attention is analog computing. Advancements in materials science and device physics have led to the development of analog Compute-In-Memory (CIM) architectures [7]. This paradigm shifts computation directly onto memory elements, drastically reducing data movement [8]. Advancements of non-volatile resistive memory technologies, particularly memristors (or Resistive RAM - ReRAM), organized into crossbar arrays led to the evolution of this architecture [9]. Memristors are variable resistor devices that can act as memory by changing their conductance values. Through ongoing advancements, the number of unique conductance values that a single memristor device can represent has progressively increased, with milestones demonstrating 2 bits [10], 5 bits [11], 9 bits [12], and ultimately 11 bits [13]. The precision of these unique values is limited by reading noise, writing variabilities, conductance drift, retention failure, and programming inaccuracies [14]–[19]. Advances in techniques to overcome these challenges allowed a progressive increase in precision. Use of an error compensation technique across multiple (no more than five) arrays achieved double precision [20]. These advancements highlight the potential of analog computing to perform computations with accuracy comparable to digital computing.

Analog computing systems, particularly those leveraging memristor-based compute-in-memory architectures, have shown promise in performing matrix-vector multiplication (MVM) efficiently, potentially reducing computational complexity and energy consumption [21]. The crossbar arrays in

Osama Abdelaleim (email:oabdelal@purdue.edu), is a doctoral candidate at the Lyles School of Civil and Construction Engineering, Purdue University, West Lafayette, Indiana, USA

Arun Prakash and Ayhan Irfanoglu are with the Lyles School of Civil and Construction Engineering, Purdue University, West Lafayette, Indiana, USA

Veljko Milutinovic is with the School of Electrical Engineering, University of Belgrade, Belgrade, Serbia

the architecture naturally implement MVM, a core operation in many linear system solvers, by leveraging fundamental physical principles like Ohm's Law and Kirchhoff's current law [22]. The complexity of MVM operation using memristors in the crossbar architecture is $O(1)$ compared to $O(n^2)$ in digital computing [7]. Researchers report that a MVM CIM circuit can achieve 100x more energy efficiency than GPUs [23].

Solving linear systems ($Ax = b$) using analog CIM has consequently gained a lot of attention, precisely because it relies heavily on MVM and demands high precision. These analog designs can be grouped into three classes: hybrid solvers, dynamical solvers, and direct feedback solvers. The hybrid (digital and analog) systems solve linear equations iteratively using MVM circuits. Progression of research in hybrid systems can be observed in the increasing integration of analog components within digital computers: ranging from the use of analog CIM as a quick generator of an initial guess for a digital solver [24], to the implementation of analog preconditioners [25], and to accelerating all MVM operations within conventional iterative algorithms like the generalized minimum residual (GMRES) [26]. These systems show potential in accelerating the MVM part of algorithms by reducing run-time by up to 1500x and saving energy by 8.5x compared to digital computing [24].

The second class of analog designs is dynamical systems, which convert the system of linear equations to a system of differential equations (DEs) whose steady-state solution is the solution of the linear system of equations. Analog systems are transient systems best described using partial differential equations (PDEs) and ordinary differential equations (ODEs). Researchers use analog integrator circuits to solve the equivalent system of DEs [27], [28], while other researchers utilize transconductance devices in their designs to solve the DEs [29], [30]. The main drawback of these systems is that, by converting the linear system into DEs, the solution can have a long settling time as it depends on dynamic components such as operational amplifiers and capacitors.

The third class of analog designs is the direct feedback methods. The goal of these systems is to achieve one-step solutions where the solution time is independent of the size of the system. Utilizing the MVM crossbar architecture in feedback using Transimpedance Amplifiers (TIA) can solve positive definite (PD) matrices in one step [31]. For sparse systems, the direct CIM design is shown to have a complexity that is independent of the matrix size (n) and given by $O(1/\lambda_{min})$ where λ_{min} denotes the minimum eigenvalue of the matrix [32]. In comparison, the complexity of solving sparse matrices by digital computing using Conjugate Gradient method is $O(n)$ and by quantum computing it is $O(\kappa^2 \log(n))$ where κ denotes the condition number of the matrix [32]. For more general matrices, complexity of the direct feedback analog computing is independent of matrix size but quadratic in the condition number ($O(\kappa^2)$) [33]. These designs contain active components that can still result in long settling time that is problem-dependent.

A common characteristic across many of these analog solver architectures, particularly those relying on dynamical

systems or feedback loops incorporating active components, is the presence of inherent settling times. Whether due to explicit time constants (RC) in dynamical systems, the propagation delays, the finite gain-bandwidth product of operational amplifiers used in feedback and peripheral circuits, or the convergence time of the implemented algorithm itself, the analog computation requires long settling time to converge to the final solution. This settling time can depend on the system size, matrix properties (e.g., condition number), and circuit non-idealities, potentially limiting the achievable speedup, especially compared to the near-instantaneous potential of passive MVM.

B. Novel Approach Using Configurable Network of Resistors

Here we introduce a fundamentally different analog CIM design for solving symmetric linear systems of equations at unprecedented speed. Instead of modeling the mathematical process of solving a linear system of equations, the proposed analog design is constructed to directly map the given linear system of equations $Ax = b$ into a resistive network. The configuration and conductance values of this network are derived directly from the matrix A and the vector b . The governing equations of the resistive network in this design are the given linear equations, and the set of nodal voltages in the network is the solution vector of the given linear system.

First, a preliminary circuit design based on direct mapping is developed to solve a $n \times n$ symmetric positive-definite (SPD) matrix system of equations. However, the speed and accuracy of the solution are limited by the number of positive off-diagonal values (up to $(n^2 - n)/2$ values). The reason is that the circuit resulting from mapping the positive off-diagonal terms contains active components, namely operational amplifiers in a negative feedback loop, whereas the negative off-diagonal term is mapped directly into a passive resistor. The proposed design transforms the $n \times n$ SPD system to a $2n \times 2n$ SPD system with at most n positive off-diagonal values without adding extra computations. Solving the transformed system is shown to require fewer components in the circuitry, speed up the convergence by orders of magnitude, consume less power, and allow the design to utilize the MVM architecture.

For the class of Symmetric Diagonally Dominant (SDD) systems, the mapping of the transformed system results in a purely passive resistive network, where the solution is achieved near-instantaneous $O(1)$. For the broader SPD class, the mapping of the transformed system results in a resistive network that includes active components, particularly operational amplifiers in negative feedback. The speed and accuracy of the solution in this case depend on the properties of the matrix A such as the maximum off-diagonal term, but, critically, remain independent of the size of the matrix.

The article is divided into five sections. Section II presents the underlying theory of representing a linear system of equations with an equivalent network of resistors. Section III details the preliminary design of the analog circuit to solve n unknowns along with its performance in terms of stability and settling time. Section IV presents the proposed design that models $2n$ unknowns detailing improvements in

speed, number of circuit components, and power consumption without affecting stability. Finally, Section VI summarizes the advantages and limitations of the proposed design.

II. BACKGROUND

The proposed design aims to construct a circuit comprising a network of resistors corresponding to an $n \times n$ linear symmetric positive-definite system of equations:

$$Ax = b. \quad (1)$$

We first present how such a system of equations may be represented as a circuit and then discuss the necessary modifications to it to account for the presence of negative resistance values.

A. Equivalent Resistive Network

A symmetric system of equations can be modeled using weighted undirected graphs and resistive networks [34]. In this representation, the network comprises n nodes, where each element of the unknown vector x corresponds to the voltage at a node, and each element of the known vector b represents the external current supplied to the corresponding node. The matrix A represents the conductance matrix, assembled from the conductance values of the resistors that connect the nodes and the resistors that connect the nodes to the ground.

Consider the example shown in Figure 1. The system of equations corresponding to the circuit shown in Figure 1 is the following 3x3 system:

$$\begin{bmatrix} k_{01} + k_{12} + k_{13} & -k_{12} & -k_{13} \\ -k_{12} & k_{12} + k_{23} & -k_{23} \\ -k_{13} & -k_{23} & k_{03} + k_{13} + k_{23} \end{bmatrix} \begin{Bmatrix} x_1 \\ x_2 \\ x_3 \end{Bmatrix} = \begin{Bmatrix} b_1 \\ b_2 \\ b_3 \end{Bmatrix} \quad (2)$$

Note that, for a resistor k_{ij} connected to nodes i and j in the circuit, Ohm's law governs the current flowing out of these nodes and through the resistor as:

$$\begin{bmatrix} k_{ij} & -k_{ij} \\ -k_{ij} & k_{ij} \end{bmatrix} \begin{Bmatrix} x_i \\ x_j \end{Bmatrix} = \begin{Bmatrix} i_i^{el} \\ i_j^{el} \end{Bmatrix}, \quad (3)$$

where k_{ij} is the conductance of the resistor between nodes i and j , x_i and x_j are the voltage at nodes i and j , respectively, and i_i^{el} and i_j^{el} are the currents flowing out of nodes i and j , respectively. Similarly, the current i_i^{el} flowing out of node i due to a resistor connected between node i and the ground is obtained as follows:

$$k_{0i} x_i = i_i^{el}, \quad (4)$$

where k_{0i} is the conductance of the resistor between node i and the ground. The resistive network satisfies Kirchhoff's current law (KCL), requiring that the summation of the current flowing out of each node i be equal to the external current b_i flowing into the node. Assembling the resistor Eqs. (3)-(4), for each resistor in the network, one obtains the system in Eq. (2). This system is easily solved by simply measuring the voltage at all the nodes that represent the unknowns x_i .

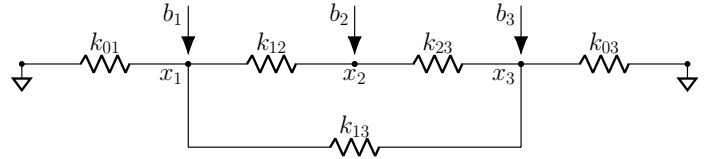


Fig. 1. Resistive network for a 3x3 system $Ax = b$. The unknown vector x represents the voltage at the nodes, while the right hand side vector b represents the external current going in to the nodes. The matrix A represents the conductance of the resistors between the nodes.

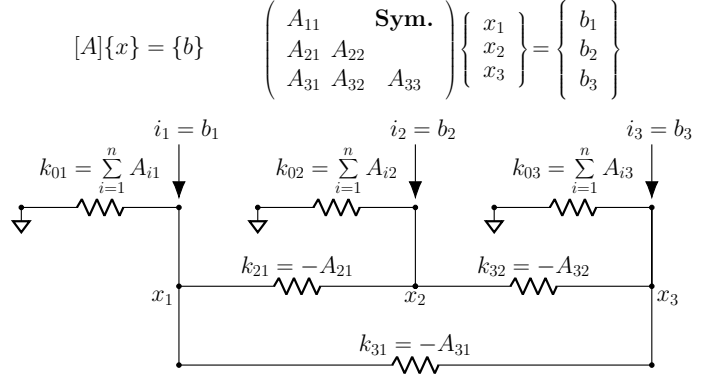


Fig. 2. Resistive network for a 3x3 system $Ax = b$. The unknown vector x represents the voltage at the nodes, while the right hand side vector b represents the external current going into the nodes. The matrix A represents the conductance of the resistors between the nodes.

In this formulation, the off-diagonal terms of the resulting matrix A are the negative of the conductance values between the corresponding nodes, while the sum of each column of the matrix A is the conductance value of the resistor connecting the corresponding node to the ground. Thus, given a symmetric system of equations $Ax = b$, the equivalent resistive network can be constructed by computing the conductance of the resistors as follows:

$$k_{ij} = -A_{ij} \quad \text{for } i \neq j, \quad (5)$$

$$k_{0i} = \sum_{j=1}^n A_{ji}, \quad (6)$$

where A_{ij} is the element at row i and column j of the given matrix A . The representation of a given symmetric system of equations by a resistive network is shown in Figure 2. The above equations show that the conductance of the resistors can be either negative or positive. A positive conductance is represented with a standard resistor, while the negative conductance is represented by the negative resistance circuit shown in Section II-B.

B. Negative Resistance Circuit

Negative resistance can be realized by designing a circuit that reverses the direction of current flow between two nodes. Such a concept has previously been employed to solve non-homogeneous differential equations [35]. To improve both accuracy and computational speed, we propose an alternative design. This proposed design extends the traditional Non-inverting operational amplifier configuration. The traditional

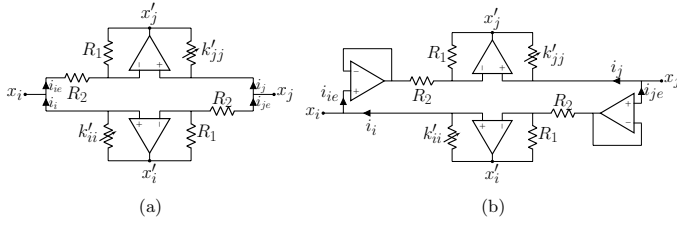


Fig. 3. Negative Resistance Circuit (a) without buffers $i_{ie} \neq 0, i_{je} \neq 0$ and (b) with buffers $i_{ie} = i_{je} = 0$

configuration is used to reverse the current between a node and the ground, whereas the proposed design can be used to reverse the current between any two nodes.

Consider the negative resistance between nodes i and j with a conductance of k_{ij} , where the voltage at nodes i and j are denoted by x_i and x_j . Instead of directly connecting the two nodes with the resistor k_{ij} , this design creates two nodes i' and j' such that node i is connected to node i' by the resistor k'_{ii} and node j is connected to node j' by the resistor k'_{jj} . The conductance of the new resistors and the voltage of the two new nodes are designed to be as follows:

$$k_{ij} = k'_{ii} = k'_{jj} \quad (7)$$

$$x'_i = x_j + 2(x_i - x_j) \quad (8)$$

$$x'_j = x_i + 2(x_j - x_i) \quad (9)$$

These equations guarantee that if x amount of current is to flow out of node i into node j in the case of normal resistor k_{ij} , the same x amount of current will flow into node i from node i' and the same x amount of current will flow out of node j into node j' . The current flowing out of nodes i and j in the negative resistance design is as follows:

$$i_i = k'_{ii}(x'_i - x_i) = -k_{ij}(x_j - x_i) \quad (10)$$

$$i_j = k'_{jj}(x'_j - x_j) = -k_{ij}(x_i - x_j) \quad (11)$$

To create the two nodes i' and j' , the Non-inverting Operational Amplifier configuration is used as shown in Figure 3 with negative feedback loop. The two resistors R_1 and R_2 are chosen to have equal conductance to have a gain of 2. The circuit in Figure 3 shows the amplifier circuits together with the two resistors k'_{ii} and k'_{jj} . Buffer circuits are added to stop unaccounted currents from being drawn from/ supplied to the nodes where computed currents will be drawn from/ supplied to. The modified circuit that includes the two buffer circuits is shown in Figure 3.

III. PRELIMINARY DESIGN: n -UNKNOWNNS

In this design, the given symmetric system of equations $Ax = b$ is mapped to an equivalent system of resistors, where the unknown vector x represents the voltages at the nodes. To simplify the system and avoid incorporation of active dynamic components, the right-hand-side vector b is not directly assigned as the supplied current. Instead, a diagonal matrix K_s , with strictly nonnegative coefficients, is introduced. This matrix represents the conductance of the resistors that connect the supply nodes to the nodes corresponding to the

$$[A]\{x\} - [K_s]\{x\} = \{b\} - [K_s]\{x\} \quad \{b\} = [K_s]\{x_s\}$$

$$\begin{pmatrix} A_{11} - k_{s1} & & \\ & \text{Sym.} & \\ A_{21} & A_{22} - k_{s2} & \\ A_{31} & A_{32} & A_{33} - k_{s3} \end{pmatrix} \begin{pmatrix} x_1 \\ x_2 \\ x_3 \end{pmatrix} = \begin{pmatrix} k_{s1}(x_{s1} - x_1) \\ k_{s2}(x_{s2} - x_2) \\ k_{s3}(x_{s3} - x_3) \end{pmatrix}$$

$$x_{si} = \begin{cases} +4V & b_i > 0 \\ -4V & b_i < 0 \\ \text{NC} & b_i = 0 \end{cases} \quad K_s = \begin{pmatrix} k_{s1} & & 0 \\ & k_{s2} & \\ 0 & & k_{s3} \end{pmatrix}$$

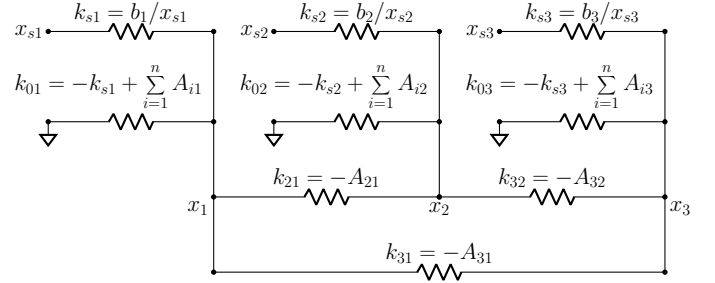


Fig. 4. Resistive network for a 3x3 system $(A - K_s)x = b - K_sx$. The current sources are replaced with voltage sources and resistors.

unknowns. These resistors have conductance values denoted as k_{si} . The introduction of K_s modifies the original system by subtracting this matrix from both sides of the equation, resulting in the following form:

$$(A - K_s)x = b - K_sx \quad (12)$$

The vector b is redefined as $b = K_sx_s$, where x_s represents the voltage vector of the supply nodes. These supply voltages, x_{si} , are connected to their respective unknown node voltages x_i through resistors with conductance k_{si} . The representation of a given symmetric system of equations by a resistive network using the preliminary design is illustrated in Figure 4.

A. Right-Hand-Side: $(b - K_sx)$

The right-hand side of the new system represents the current flowing from the supply nodes, which can be adjusted by controlling either the voltage of the supply nodes or the conductance of the associated resistors. In this design, the voltages of the supply nodes are kept constant and the vector b is mapped by varying the conductance of the supply resistors. This choice eliminates the need for a Digital-to-Analog Converter (DAC) and simplifies the implementation, as the control of variable resistors is also needed for the left-hand-side.

The supply nodes are selected to be either $x_s^+ = 4V$ or $x_s^- = -4V$. Each unknown node i with voltage x_i is connected to the Drain terminal (D) of a digitally controlled analog switch through a variable resistor with conductance k_{si} . The operation of the switch is controlled by two digital signals:

- 1) **Enable Terminal (EN):** Connected to the digital bit b_{i-on} . If the corresponding element of the vector b is zero, b_{i-on} is set to digital zero, causing the switch to remain open and isolating the node i from any supply node.

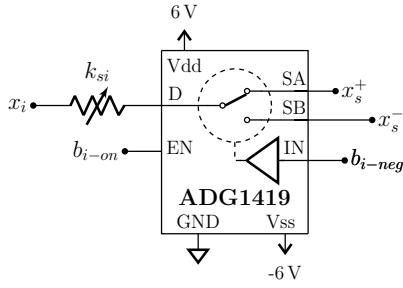


Fig. 5. Right-Hand-Side Circuit for each node. Each node i is connected to a supply resistor of conductance k_{si} that is connected to either x_s^+ in case b_i is positive or x_s^- in case b_i is negative. In the case of $b_i = 0$, the switch is not enabled.

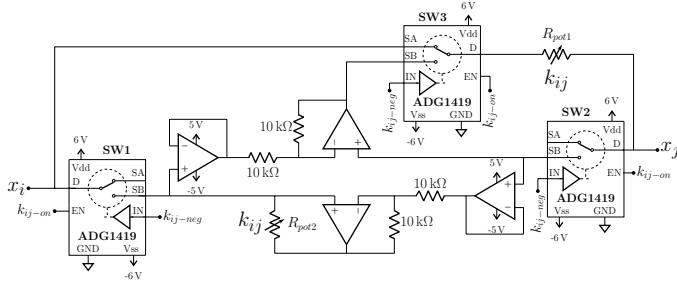


Fig. 6. Element Circuit. The three switches are enabled when the required conductance k_{ij} between node i and j is not zero. If k_{ij} is positive the active circuit becomes only the resistor R_{pot1} connecting nodes i and j . If k_{ij} is negative the active circuit becomes the negative resistance circuit between nodes i and j .

- 2) **Control Terminal (IN):** Connected to digital bit b_{i-neg} . This bit determines whether the node is connected to x_s^+ (positive supply) via the Source A terminal (SA) for positive elements of b or to x_s^- (negative supply) via the Source B terminal (SB) for negative elements of b .

The conductance of each supply resistor, k_{si} , is computed as follows:

$$k_{si} = b_i/x_{si} = |0.25b_i| \quad (13)$$

This computation can be done digitally by two-bit shift or by directly connecting the bits to a digital potentiometer with two-bit shift. An example of the right-hand-side circuit for node i is shown in Figure 5.

B. Left-Hand-Side: $(A - K_s)x$

The left-hand side of the new system represents the conductance matrix of the resistive network, where each resistive element in the circuit can exhibit either positive or negative resistance. To ensure the generality of the circuit and its ability to represent any symmetric system of equations, this design employs digitally controlled analog switches to toggle between a normal variable resistor (positive resistance) and a negative resistance circuit for each element of the system, as shown in Figure 6.

For each resistive element in the matrix $(A - K_s)$, the resistance values of the variable resistors R_{pot1} and R_{pot2} are set to be the absolute value of the inverse of the corresponding conductance calculated by Equations 5 and 6. Two additional control bits are associated with each resistive element:

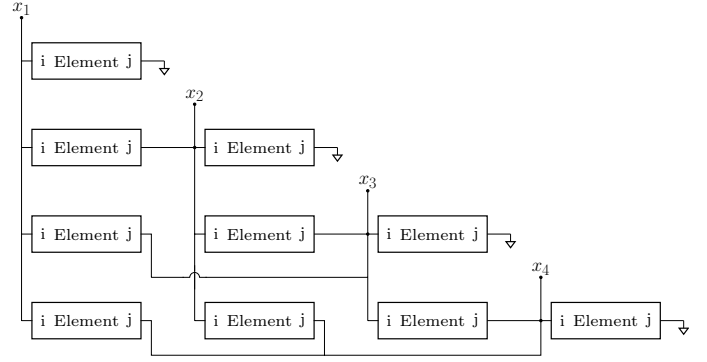


Fig. 7. The assembly of the Left-Hand-Side Circuit. Each element has digital inputs representing k_{ij-on} , k_{ij-neg} , and k_{ij} .

- 1) **Activation Bit (k_{ij-on}):** This bit determines whether the resistive element is active (i.e., has nonzero conductance). It is connected to the Enable (EN) terminals of the three switches within the element circuit.
 - when $k_{ij-on} = 0$, the switches remain open, disconnecting nodes i and j , effectively removing the element from the circuit.
 - when $k_{ij-on} = 1$, the switches close, connecting the Drain terminal (D) to either the Source terminal A (SA) or the Source terminal B (SB), depending on the second control bit.
- 2) **Polarity Bit (k_{ij-neg}):** This bit determines whether the element represents a positive or negative resistance. It is connected to the control terminals (IN) of the three switches within the element circuit.
 - when $k_{ij-neg} = 0$, the switches configure the circuit for positive resistance. The Drain terminal (D) of the switches are connected to the Source terminal A (SA), establishing a connection between nodes i and j only through the variable resistor R_{pot1} . In this configuration, switch SW3 closes to activate the positive resistance path, while switches SW1 and SW2 remain open, isolating the negative resistance circuit.
 - when $k_{ij-neg} = 1$, the switches configure the circuit for negative resistance. The Drain terminal (D) of the switches are connected to the Source terminal B (SB), engaging the negative resistance circuit between nodes i and j .

The assembly of the left-hand-side of the design closely resembles a lower triangular matrix, reflecting the symmetry of the system. Each element in the off-diagonal of the linear system corresponds directly to an element circuit connecting the same pair of nodes. For instance, the element in row 2, column 3 of the matrix and the layout is represented by an element circuit between the unknowns x_2 and x_3 . The diagonal elements in this layout represent the elements between the unknown x_i and the ground. This structured layout helps visualizing the relation between the circuit elements and the matrix elements. An example of the assembly of the left-hand-side of this design for a 4x4 system is shown in Figure 7.

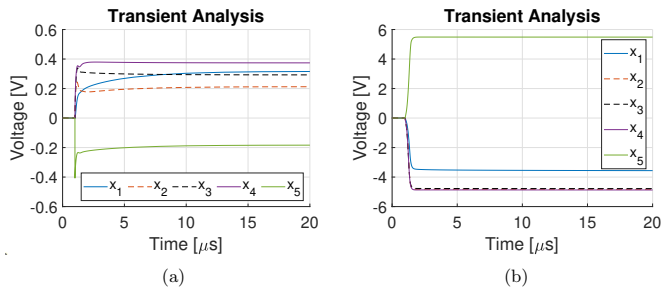


Fig. 8. Transient Analysis of two 5x5 systems using the preliminary design. Plot (a) shows a stable solution for a Positive Definite matrix ($Ax = b$). Plot (b) shows unstable solution for a Negative Definite matrix ($-Ax = -b$). The theoretical solution of both systems is $x = [0.32 \ 0.21 \ 0.29 \ 0.37 \ -0.18]^T$.

C. System Testing

To evaluate the performance of the system, random symmetric matrices of varying sizes were generated using MATLAB R2022a [36] and then simulated in LTspice v17.1 [37]. The simulations were transient analysis simulations, where the supply voltage was modeled as a step function that transitions from zero to x_s^+ or x_s^- at $1 \mu s$. This setup was used to analyze the system settling time and the accuracy of the solution for the unknown vector x . The observed performance of the preliminary design across different subdomains of the linear system of equations $Ax = b$, is summarized as follows:

1) Unsymmetric Systems:

These systems cannot be represented by the circuit. A transformation is required to convert such systems into Symmetric Positive Definite (SPD) systems. One potential transformation, though computationally expensive, is $A^T Ax = A^T b$.

2) Symmetric Non-Positive-Definite Systems:

While these systems can be represented by the circuit, the system does not converge to the expected solution. In such cases, the voltage at the output node of at least one operational amplifier (opamp) in the negative resistance circuits reaches the amplifier maximum or minimum output voltage. This saturation indicates a positive feedback loop that results in circuit instability. This instability observation can be explained by using the analogy between resistive networks and spring networks as presented in [38]. In mechanical systems, a non-positive eigenvalue in the stiffness matrix (analogous to the conductance matrix) signifies instability, where small perturbations in displacement (analogous to voltage) result in unbounded motion.

A test case for a 5x5 system is illustrated in Figure 8. The system is symmetric positive definite and is solved in two scenarios. The first plot presents the solution for the original system, while the second plot shows the results of the negative definite system obtained by multiplying both the conductance matrix A and the vector b of the original system by -1 . In theory, the expected solution for both systems should be identical. The solution vector for the systems is

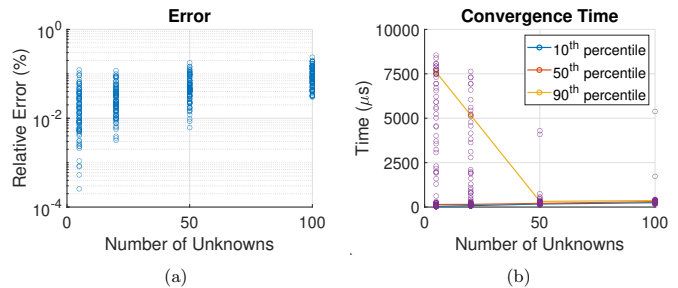


Fig. 9. Analysis of 400 random systems using the preliminary design. Plot (a) shows the maximum error between the converged solution and the theoretical values of each system. Plot (b) shows the maximum convergence time for each system

$x = [0.32 \ 0.21 \ 0.29 \ 0.37 \ -0.18]^T$. The Negative Definite system exhibits instability, whereas the Positive Definite system demonstrates a stable solution with a maximum error of less than 0.01% relative to the expected solution.

3) Symmetric Positive-Definite Systems:

These systems can be represented by the circuit, and the circuit converges to the expected solution. The accuracy of the solution depends on the specifications of the opamps and variable resistors used. For systems where at least one conductance value is negative, the active circuit of the system includes opamps that require a settling time before stabilizing.

To evaluate convergence time and error in this domain, random symmetric systems of varying sizes were generated and simulated. The conductance matrices, created using MATLAB's "sprandsym" function, are full matrices with eigenvalues ranging between and including $10 \mu S$ and $1000 \mu S$. For each generated system, the unknowns x_i were randomly assigned within $[-0.5V, 0.5V]$, and the corresponding b vector was computed by $b = Ax$. An equivalent circuit for each generated system was modeled and simulated in LTspice v.17.1.8 software using the AD712 model for the opamps through two analyses:

- **Operating Point Analysis:** The supply nodes had constant voltage of x_s^+ and x_s^- . This analysis provided the expected converged solution for the circuit. The maximum error in the converged solution of each generated system is shown in Figure 9. In all simulated systems, the expected errors from using this design is less than 0.3%.
- **Transient Analysis:** The supply voltage was modeled as a step function transitioning to x_s^+ and x_s^- at $1 \mu s$. Convergence time was defined as the time instant beyond which the voltages are always within 1% of the operating point solution. Results, presented in Figure 9, show median convergence times ranging from $144 \mu s$ for 5x5 systems to $307 \mu s$ for 100x100 systems. However, the 90th percentile times range from $7600 \mu s$ to $370 \mu s$, reflecting large variability (an order of magnitude difference).

This variability complicates determining when to read reliably the solution in practical applications and highlights the need for a better design in this domain.

4) Positive Weighted Undirected Graph Systems:

A subset of symmetric positive definite systems, these systems can be decomposed into the sum of a Laplacian matrix and a diagonal matrix with strictly positive values. The active circuit for such systems consists solely of positive resistors, enabling a purely resistive network. As a result, the solution is achieved at the theoretical maximum speed determined by the current flow in the network ($O(1)$) regardless of the problem size. The accuracy in this case depends solely on the specifications of the variable resistors.

IV. PROPOSED DESIGN: $2n$ -UNKNOWN

The primary motivation for this design is to reduce the number of components in the circuit, increase the range of problems that can be represented using strictly positive resistance, and reduce the settling time of the circuit. The design achieves this by transforming the original $n \times n$ system of equations into a new $2n \times 2n$ system that ensures that most resistive elements are positive, without introducing significant additional digital computations. The transformed system is expressed as:

$$\begin{bmatrix} K_A & K_B \\ K_B & K_A \end{bmatrix} \begin{Bmatrix} x \\ -x \end{Bmatrix} = \begin{Bmatrix} b - K_s x \\ -b - K_s(-x) \end{Bmatrix}, \quad (14)$$

where K_A and K_B are $n \times n$ sub-matrices defined as:

$$K_A = D + 0.5(A - |A|) - K_s \quad (15)$$

$$K_B = D - 0.5(A + |A|). \quad (16)$$

where D is a diagonal matrix with strictly non-negative elements. This transformation ensures that the off-diagonal terms of the sub-matrices K_A and K_B are negative, corresponding to positive resistive elements in the circuit. Importantly, no additional computations are required for these values, as they directly correspond to the off-diagonal terms of the original A matrix, although assigned between different nodes. For positive resistive element between nodes i and j in the original system, the transformed system retains the same positive resistance between these nodes. Additionally, it introduces another positive resistive element with identical conductance between nodes $n+i$ and $n+j$. For negative resistive elements between nodes i and j in the original system, the transformed system replaces the negative resistance with two positive resistive elements of the same conductance. One resistor connects nodes i and $n+j$, while the other connects nodes j and $n+i$.

A. D -Matrix

The choice of matrix D plays a pivotal role in determining the domain of symmetric linear systems that will be positive definite in the transformed system and, therefore, solvable. In addition, it influences both the speed and the accuracy of the solution. A comparable, though less practical, transformation was proposed for support trees [34]. In that approach, D is

selected as the diagonal of the original matrix A , and K_s is set to the zero matrix. However, such approach does not guarantee that a positive definite system will remain positive definite after transformation, thereby reducing the range of problems that can be addressed.

1) *Stability Condition:* To ensure the stability of the system, it is essential to analyze the conditions under which the transformed system remains positive definite, as this is a key criterion for stability. Using the theorems for the determinants of block matrices [39], the eigenvalues λ of the transformed system, for any choice of D , is derived. The eigenvalues are computed as follows:

$$\det \left(\begin{bmatrix} K_A - \lambda I_n & K_B \\ K_B & K_A - \lambda I_n \end{bmatrix} \right) = \det(K_A + K_B - \lambda I_n) \det(K_A - K_B - \lambda I_n) \quad (17)$$

Thus, positive definiteness of the system is achieved if both matrices $(K_A - K_B)$ and $(K_A + K_B)$ are positive definite. These matrices can be expressed and simplified as follows:

$$K_A - K_B = A - K_s, \quad (18)$$

$$K_A + K_B = 2D - |A| - K_s. \quad (19)$$

The condition expressed in Equation 18 requires that the original system $(A - K_s)$ be positive definite. To preserve the positive definiteness of the transformed system, the matrix D is chosen to ensure that $(K_A + K_B)$ is diagonally dominant, making it positive definite. Since $(K_A + K_B)$ can be decomposed as the sum of a diagonal matrix D with strictly positive elements and a matrix $(-|A| - K_s)$ with strictly non-positive elements, achieving diagonal dominance requires that the sum of each column of $(K_A + K_B)$ be greater than zero. This requirement leads to the following condition for each element of the matrix D :

$$D_{ii} > \frac{1}{2} \left[(K_s)_{ii} + \sum_{j=1}^n |A_{ji}| \right] \quad (20)$$

2) *Scaling:* To optimize the design for the choice of D , its effect on both the accuracy and speed of the expected solution was studied. In this study, D was selected as a scaled identity matrix, with the scaling determined as the maximum value of the sums of the columns of the absolute value of the conductance matrix A as follows:

$$D = \beta \max_i \left(\sum_{j=1}^n |A_{ji}| \right) I_n, \quad (21)$$

where β is a scaling factor with $\beta \geq 0.5$ to satisfy the condition in Equation 20.

Random symmetric positive definite matrices, not diagonally dominant, with variable sizes were generated and simulated for various values of β . The results consistently showed that reducing β significantly decreased both the error and the convergence time, as illustrated for two example systems in Figure 10. Thus, minimizing D while ensuring that the system remains positive definite is favorable for accuracy and performance.

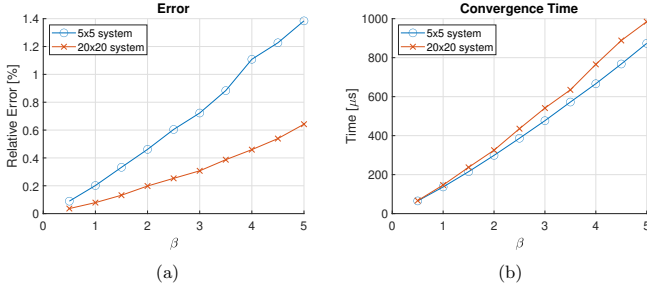


Fig. 10. Analysis of two random systems using the proposed design for different values of D matrix scaling β . Plot (a) shows the maximum error between the converged solution and the theoretical values of each system. Plot (b) shows the maximum convergence time for each system.

3) *Proposed D-Matrix*: The selection of D was further refined using an analogy between resistive networks and 1D spring systems. A conductance (stiffness) matrix A with a zero determinant (at least one zero eigenvalue) corresponds to a spring system without supports, making it unstable. In a resistive network (1D Spring System), this instability occurs when the sums of the columns in the matrix are zero. Stability can be achieved by ensuring that at least one column sum is positive, akin to providing a single support in a mechanical system.

To stabilize the system, the diagonals of D were chosen as:

$$D_{ii} = \begin{cases} (K_s)_{ii} + \frac{1}{2} \left[\sum_{j=1}^n |A_{ji}| \right] & \text{for } i = 1 \\ \frac{1}{2} (K_s)_{ii} + \frac{1}{2} \left[\sum_{j=1}^n |A_{ji}| \right] & \text{for } i \neq 1 \end{cases} \quad (22)$$

This choice ensures that the sum of each column in the matrix ($K_A + K_B$), except for the first column, is zero. It also simplifies the design by ensuring that only nodes 1 and $n + 1$ are connected to the ground. The conductance between these nodes and the ground is k_{s1} , which is the conductance of the resistors connecting these nodes to the supply node x_s .

The choices for the system transformation in the proposed design do not introduce additional digital computations beyond those required in the preliminary design. The resistive network for the proposed design is constructed with conductance values assigned as:

$$k_{ij} = \begin{cases} k_{s1} & \text{for } i = 0, \\ & \text{and } j = 1, n + 1 \\ -A_{ij} & \text{for } j < i, A_{ij} < 0 \\ & \text{and } i = 1, \dots, n \\ A_{ij} & \text{for } j < i, A_{ij} > 0 \\ & \text{and } i = 1, \dots, n \\ A_{ii} - \frac{1}{2} \left(k_{s1} + \sum_{c=1}^n |A_{ci}| \right) & \text{for } j = n + i \\ & \text{and } i = 1, \dots, n \\ 0 & \text{for all other elements} \end{cases} \quad (23)$$

This approach optimizes the stability, accuracy, and convergence speed of the system while minimizing unnecessary complexity in the design.

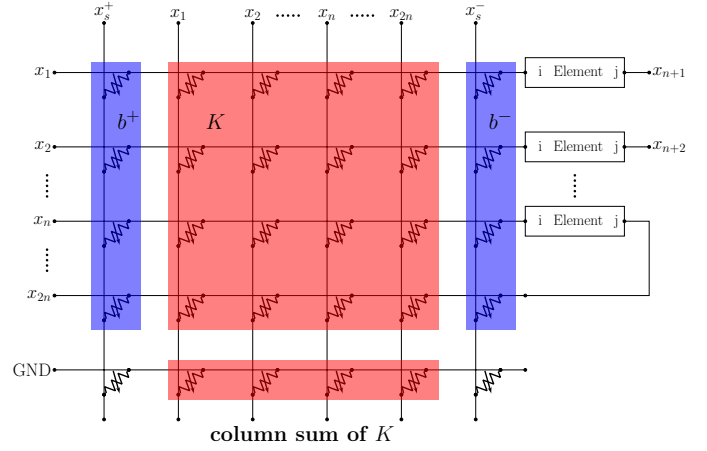


Fig. 11. Proposed design in cross-point architecture

4) *Cross-point Architecture*: One notable advantage of the proposed design is its compatibility with a cross-point architecture, as shown in Figure 11, the same architecture widely used for Matrix Vector Multiplication (MVM). In this setup, the rows and columns of the array represent the voltages of the unknown vector x , with each row directly connected to the corresponding column. In addition, two additional columns are introduced for the supply nodes x_s^+ and x_s^- , and an additional row is added for the ground node.

The elements of the transformed matrix K correspond to the conductance values between the various nodes in the unknown vector x . Theoretically, only half of the elements in the cross-point array are needed to represent the system due to symmetry. However, to maintain the matrix structure in the array for MVM operations, the off-diagonal terms of the submatrices K_A and K_B are divided by 2. These values are then assigned symmetrically to the elements k_{ij} and k_{ji} , effectively splitting the original resistors into two parallel resistors.

The diagonal elements of the transformed matrix K , whether assigned within the array or not, do not influence the design, as both ends of these resistors are connected to the same node, rendering them effectively nonexistent. Furthermore, the diagonals of the submatrix K_B are deliberately set to zero in the array, as these elements can represent either positive or negative resistance. External element circuits are used to connect each node i to node $n + i$, enabling flexible resistance representation while preserving the structure of the array for MVM operations.

The elements of the supply matrix K_s are assigned to the conductance values in the two additional columns, based on the sign of the corresponding element in the right-hand-side vector b . The conductance values are calculated using Equation 13. The additional row in the system includes the conductance values calculated as the sums of the columns of the transformed matrix K .

B. System Testing

To evaluate the performance of the proposed design, the same procedure as that used for the preliminary design was

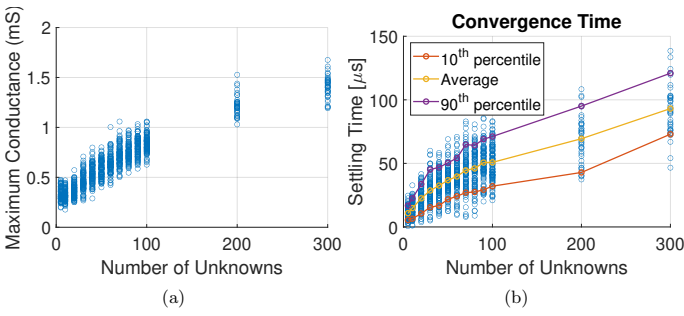


Fig. 12. Analysis of 1200 random systems (density=1) using the proposed design. Plot (a) shows the maximum conductance in the transformed system of each system. Plot (b) shows the maximum convergence time for each system

applied. Random symmetric matrices of varying sizes were generated using MATLAB and then simulated in LTspice v17.1. The simulations were transient analysis simulations, where the supply voltage was modeled as a step function that changes from zero to x_s^+ or x_s^- at $1 \mu s$. This setup was used to analyze the system's settling time and the accuracy of the solution for the unknown vector x . By design, the domain of stable solutions for the proposed design corresponds to the domain of symmetric positive definite matrices.

The proposed design ensures positive resistance in all elements, except those represented by the diagonal elements of the submatrix K_B . The domain of matrices that maintains strictly positive resistance can be identified as the domain of matrices that have nonpositive diagonals of K_B after transformation. This condition is expressed as:

$$K_{Bii} = D_{ii} - 0.5(A_{ii} + |A_{ii}|) \leq 0 \quad (24)$$

where substituting D_{ii} from Equation 22 yields:

$$A_{ii} \geq (K_s)_{ii} + \sum_{j=1, j \neq i}^n |A_{ji}| \quad (25)$$

This condition indicates that the system $(A - K_s)$ must be diagonally dominant. Consequently, solving a diagonally dominant symmetric matrix with this design achieves a complexity $O(1)$, which is the theoretical maximum speed attainable for the solution process.

1) *Complexity Studies:* To evaluate the performance of the proposed design in terms of error and speed within the domain of symmetric positive definite systems that are not diagonally dominant, both operating point and transient analyses were conducted on randomly generated systems in this domain. For each randomly generated conductance matrix A , unknowns x_i were randomly assigned values within the range $[-0.5V, 0.5V]$, and the corresponding vector b was calculated by $b = Ax$.

The first analysis focused on a set of full matrices with eigenvalues ranging between and including $10 \mu S$ and $1000 \mu S$. This set included the 400 matrices previously analyzed in Section III-C to compare the performance of the proposed design relative to that of the preliminary design. All simulated systems exhibited errors in the converged solution of less than 0.3%. The results of the convergence time analysis are presented in Figure 12. The median convergence time ranged from $10 \mu s$ for 5×5 systems to $92 \mu s$ for the 300×300 systems,

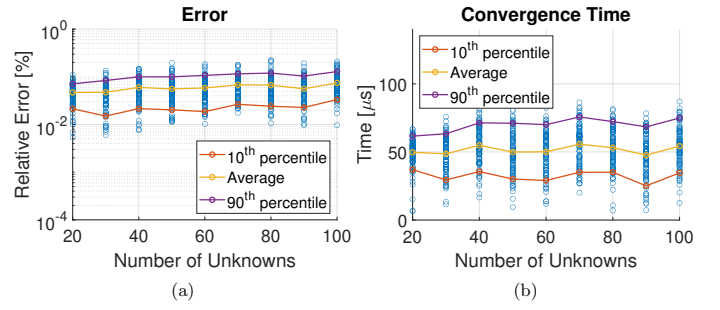


Fig. 13. Analysis of 900 systems with maximum conductance within 10% of $800 \mu S$ (density=1) using the proposed design. Plot (a) shows the maximum error between the converged solution and the theoretical values of each system. Plot (b) shows the maximum convergence time for each system

while the 90th percentile of the convergence time ranged from $17 \mu s$ to $121 \mu s$ for the same system sizes.

The proposed design demonstrated a remarkable improvement in convergence time, achieving at least a 100x speedup compared to the preliminary design. Systems that required milliseconds to solve using the preliminary design were solved in only tens of microseconds with the proposed design. Furthermore, the variation in convergence time across simulations was significantly reduced, highlighting the efficiency and consistency of the proposed design. Although the results in Figure 12 suggest a linear relationship between the settling/convergence time of the systems and the number of unknowns, the generated systems also exhibit a linear dependency between the number of unknowns and the maximum conductance in the transformed system. This indicates that the settling time may be influenced by either the number of unknowns or the maximum conductance in the transformed system.

To determine whether the maximum conductance in the transformed system or the number of unknowns is the controlling factor for the speed and error of the design, a second test was conducted. In this test, the same procedure for generating random systems was applied, but only systems with a maximum conductance in the transformed system within 10% of $800 \mu S$ are selected. This procedure did not yield systems meeting this criterion for fewer than 20 or more than 100 unknowns. As in the previous study, these systems were full matrices with eigenvalues ranging between and including $10 \mu S$ and $1000 \mu S$. The results, presented in Figure 13, show a constant trend in both error and settling time for solving these linear systems using the proposed design. On average, the error in the converged solution for 20×20 systems is 0.05%, comparable to 0.07% for 100×100 systems. Similarly, the average settling time remains nearly constant, ranging from $50 \mu s$ for 20×20 systems to $55 \mu s$ for 100×100 systems.

To verify this observation in a wider range of unknowns, a third test was conducted. This test used a similar procedure to generate random systems with a density of 0.5 and a maximum conductance in the transformed system within 10% of $550 \mu S$. These systems, like the previous ones, had eigenvalues ranging between and including $10 \mu S$ and $1000 \mu S$. The results, shown in Figure 14, again indicate a constant trend in both error and settling time. On average, the error in the

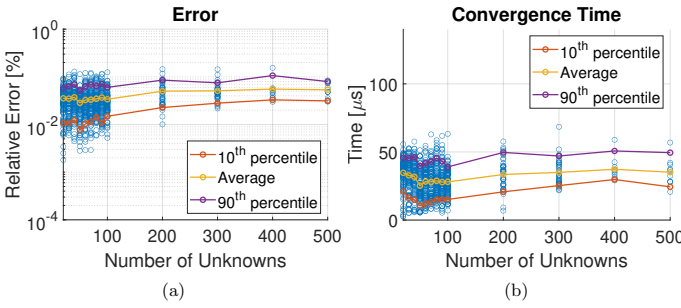


Fig. 14. Analysis of 1200 systems with maximum conductance within 10% of $550 \mu S$ (density=0.5) using the proposed design. Plot (a) shows the maximum error between the converged solution and the theoretical values of each system. Plot (b) shows the maximum convergence time for each system

converged solution for the 20x20 systems is 0.035%, similar to 0.054% for the 500x500 systems. Likewise, the average settling time is approximately $35 \mu s$ for both the 20x20 and the 500x500 systems, confirming that the settling time is largely independent of the number of unknowns.

In the proposed design, the resistors connecting the nodes to the ground are minimal or nonexistent, meaning that the maximum conductance in the transformed system corresponds to the maximum conductance of the resistors connecting the nodes representing the unknowns. This is reflected in the off-diagonal terms of the transformed matrix, which are equal to the off-diagonal terms of the original A matrix. Derived from Equations 22 and 24, the diagonal elements of the sub-matrix K_B , part of the off-diagonal terms of the transformed system, are computed assuming the diagonals of A are positive as:

$$K_{Bii} = -\frac{1}{2} \left(A_{ii} - K_{sii} - \sum_{j=1, j \neq i}^n |A_{ji}| \right) \quad (26)$$

These diagonal terms represent the deviation of the matrix $(A - K_s)$ from diagonal dominance. The complexity studies demonstrate that the speed and error in solving symmetric positive definite systems that are not diagonally dominant using the proposed design depend on key matrix properties: the eigenvalues, the maximum absolute values of the off-diagonal terms, and the deviation from diagonal dominance. Importantly, these factors show that the performance does not depend on the size of the system being solved.

2) *Operational Amplifier Specifications*: The accuracy and speed of the proposed design are influenced by the specifications of the operational amplifiers used. To examine the impact of amplifier choice, the same set of random matrices used in the preliminary design and test 1 of the complexity studies were simulated using three different amplifiers. The first amplifier, AD712, was used in all previous simulations. The second amplifier, LTC2050, features a low input offset voltage to minimize errors in the converged solutions. The third amplifier, LTC6268, has relatively high slew rate and gain bandwidth product to reduce settling time. The main specifications of these amplifiers are summarized in Table I.

The simulation results, presented in Figure 15, reveal a tradeoff between speed and accuracy. Using the LTC2050 amplifier reduces the error in the converged solution by an

TABLE I
OPERATIONAL AMPLIFIERS SPECIFICATIONS

Specification	AD712	LTC2050	LTC6268
Input Offset Voltage	1 mV	3 μV	2.5 mV
Gain Bandwidth Product	4 MHz	3 MHz	500 MHz
Slew Rate	20 V/ μs	2 V/ μs	400 V/ μs

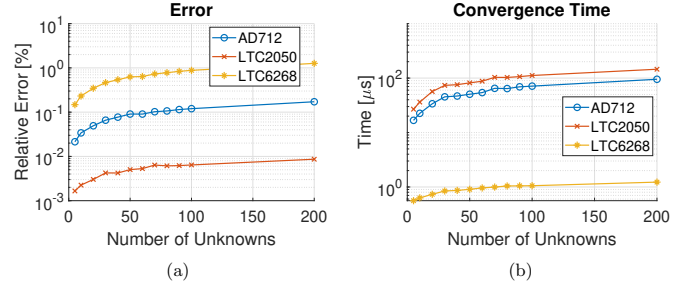


Fig. 15. Analysis of 1150 random systems (density=1) using the proposed design for different amplifiers. Plot (a) shows the 90th percentile of the maximum error between the converged solution and the theoretical values of each system. Plot (b) shows the 90th percentile of the maximum convergence time for each system

order of magnitude compared to the AD712 but increases the settling time by approximately 1.6 times. Conversely, the LTC6268 amplifier significantly speeds up the system, achieving a two-orders-of-magnitude reduction in settling time, but with an increase in error by an order of magnitude. This tradeoff highlights that a lower input offset voltage results in higher accuracy in the converged solution, while a higher gain bandwidth product leads to faster system speed.

3) *System Scaling*: The motivation behind the proposed design is to optimize performance in terms of speed, accuracy, and power consumption. A detailed analysis of the system power consumption is presented in Section IV-B4. One approach to reducing power consumption is to scale the system of equations such that the conductance values of both the left-hand and right-hand side models are proportionally scaled down. When both models are scaled by the same factor, denoted as α , the resulting solution for the unknown vector x remains unchanged. The scaled system is expressed as:

$$\alpha \begin{bmatrix} K_A & K_B \\ K_B & K_A \end{bmatrix} \begin{Bmatrix} x \\ -x \end{Bmatrix} = \alpha \begin{Bmatrix} b - K_s x \\ -b - K_s(-x) \end{Bmatrix} \quad (27)$$

To study the effect of the scaling factor α on the error and settling time, random symmetric positive definite matrices that are not diagonally dominant were generated and simulated for different values of α . Figure 16 presents results for two systems: a 5x5 system and a 20x20 system. The simulations consistently show that reducing α decreases both the error in the converged solution and the convergence time. Therefore, scaling the system down is highly advantageous, as it enhances accuracy, speeds up the solution process, reduces power consumption, and adjusts the conductance values of resistors to a commercially common range. Additionally, operating the design in the low conductance (high resistance) range

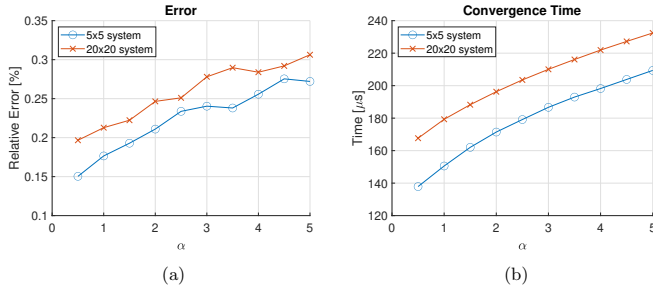


Fig. 16. Analysis of two random systems using the proposed design for different values of system scaling α . Plot (a) shows the maximum error between the converged solution and the theoretical values of each system. Plot (b) shows the maximum convergence time for each system.

minimizes errors from parasitic resistance by reducing the relative impact of parasitic resistances compared to the circuit resistors.

4) *Power Consumption*: The power consumption of the proposed design is analyzed in this section, assuming the circuit operates at the converged solution of the system. The analogy between resistors and 1D springs is employed to calculate the system power. In this analogy, the power equation for a resistor is equal to the energy equation for a spring, where the conductance of the resistor represents the stiffness of the spring, and the voltage difference across the resistor corresponds to the displacement difference between the spring's end nodes. The total energy in a spring system is calculated using the conservation of energy between the external energy (from the applied forces or the right-hand side) and the internal energy stored in the springs.

Applying this conservation principle to the proposed design, the total power P_{k+} of the left-hand-side model, assuming only positive resistors, is expressed as:

$$P_{k+} = \sum_{k=1}^{n_{el}} k_k (x_i - x_j)^2 = x_{2n}^T K_{2n} x_{2n}, \quad (28)$$

where n_{el} is the number of resistors in the left-hand-side, k_k is the conductance of the individual resistors, x_i and x_j are the voltages at the two ends of the resistor, and K_{2n} is the transformed conductance matrix of the proposed design.

Since this equation assumes all conductance values are positive, a correction term is necessary to account for negative resistance. According to the choice of the D matrix presented in Section IV-A3, negative resistance exist only between nodes i and $n+i$, where the voltage difference is $2x_i$. The power correction term P_{k-} , accounting for two resistors (R_{pot1}, R_{pot2}) with the same conductance in the negative resistance circuit, is:

$$P_{k-} = 6x^T (K_B + |K_B|) x. \quad (29)$$

The power of the remaining components of the left-hand-side model of the system is derived from analyzing the circuit in Figure 3 with buffers, where nodes i and j in this case are nodes i and $n+i$. The output voltage at the buffers are x_i and $-x_i$, while the output voltage at the opamps output are $3x_i$ and $-3x_i$. Thus, the power consumption P_R of the resistors

with conductance k_R used to control the gain of the circuit can be expressed as follows:

$$P_R = 4k_R x^T x \quad (30)$$

Combining these equations and simplifying Equation 28 using Equations 14 and 18, and adding the power consumption from the right-hand side ($2x^T K_s x$), the total system power P_{sys} is:

$$P_{sys} = P_{amp} + P_{sw} + 4k_R x^T x + 6x^T (K_B + |K_B|) x + 2x^T A x, \quad (31)$$

where P_{amp} and P_{sw} are the total power consumed by amplifiers and switches, respectively. This equation highlights that power consumption decreases for systems with lower conductance, making it advantageous to scale down the system. Additionally, the power consumption of the operational amplifiers can be further reduced by lowering the supply voltage to the amplifiers, ensuring that it remains sufficient to accurately output three times the maximum expected voltage in the solution vector.

V. DISCUSSION

This article presents two analog circuit designs, preliminary and proposed, aimed at accelerating the solution of symmetric linear systems of equations, an essential computational task in various applications. Although both designs leverage the analogy between 1D spring systems and resistive networks, the proposed design improves the process by reducing the number of circuit components by approximately 70% compared to the preliminary design, despite adding n more unknowns to the system. This reduction in components is detailed in Table II.

TABLE II
NUMBER OF CIRCUIT COMPONENTS

Number of	Preliminary Design	Proposed Design
Unknowns	n	$2n$
Variable Resistors	$n^2 + 2n$	$2n^2 + 1$
Resistors (10 kΩ)	$2(n^2 + n)$	$4n$
Analog Switches	$1.5n^2 + 2.5n$	$3n$
OpAmps	$2(n^2 + n)$	$4n$

The proposed design is tailored specifically for solving Symmetric Positive Definite (SPD) systems, which define its stable domain. Within this domain, the performance of the system varies based on the matrix properties:

- **Diagonally Dominant Systems:** For these systems, the solution is achieved with $O(1)$ complexity, irrespective of the matrix size or specific properties, since the circuit consists exclusively of resistors. This enables the system to reach the theoretical maximum speed.
- **Non-Diagonally Dominant Systems:** The accuracy and speed of the solution depend on the specifications of the opamps used and the system matrix properties such as eigenvalues, the maximum off-diagonal term, and deviation from diagonal dominance. However, for systems with similar eigenvalues and matrix properties, the solution still achieves $O(1)$ complexity.

While the proposed design excels in speed and accuracy, it faces a computational setback in calculating the sum of the absolute values of the columns, which has a complexity of $O(n^2)$. To mitigate this issue, several solutions are proposed.

- **System Assembly:** In applications such as the Finite Element Method, calculating the sum is computationally inexpensive when calculated as part of the construction and assembly of the linear system of equations
- **Parallel Resistors:** Doubling the number of variable resistors and constructing the variable resistors representing the diagonals of the submatrix K_B using individual variable resistors in parallel, each with conductance corresponding to individual elements in the corresponding column.
- **Matrix Vector Multiplication (MVM):** Utilizing an analog MVM circuit to multiply the matrix by a vector of ones, reducing the complexity of this operation to $O(1)$

VI. CONCLUSION

The presented research work introduces a fundamentally new class of analog compute-in-memory (CIM) solvers, resistive network mapping, that directly maps the given SPD system of equations into a resistive network. This mapping is only realized after leveraging the noninverting operational amplifier configuration with some modifications to map negative conductance. Another key aspect of the architecture is the proposed transformation of the original $n \times n$ system (up to $(n^2 - n)/2$ negative conductance values) into an equivalent $2n \times 2n$ system (up to n negative conductance values). Mapping and solving this transformed system reduces the needed component count by more than 70%, consumes less power, and speeds up the computation by orders of magnitude without additional computational overhead.

For the subclass of symmetric diagonally dominant (SDD) matrices, mapping the transformed system results in a purely passive resistive network whose nodal voltages settle in effectively zero time. This yields true $O(1)$ complexity where the solution speed reaches the theoretical speed limit for analog-CIM architectures and outperforms the state-of-the-art analog solvers, whose settling times are limited by RC constants and feedback loop dynamics, by orders of magnitude. Compared to conventional digital algorithms (even highly optimized sparse solvers), the passive resistive network achieves multiple orders of magnitude speedups for large SDD systems, while consuming a fraction of the energy.

More generally, for any SPD system, the solution speed remains independent of the number of unknowns and depends only on other matrix properties such as eigenvalues, maximum off-diagonal term, and deviation from diagonal dominance. The accuracy of the proposed design is limited by the specifications of the variable resistors and opamps used, which will keep improving with the rapid improvements in device technology. Numerical convergence studies of non-diagonally dominant SPD systems show four significant figure accuracy under idealized conditions. Nonetheless, the sensitivity of solution to component tolerances and environmental perturbations warrants further investigations.

A notable advantage of the proposed design is its compatibility with the cross-point architecture, commonly used in resistive memory arrays. This compatibility facilitates in-memory computations, enabling multiple operations such as MVM within the same framework.

In summary, Resistive Network Mapping presents a compelling paradigm shift in computational linear algebra by eliminating the mathematical process of solving linear systems of equations. The proposed design offers substantial improvements in speed and efficiency, particularly for SPD systems, such as those arising from Finite Element Analysis in Computational Solid Mechanics. Future work could explore extending this design to a broader range of linear systems and developing more robust solutions for handling non-positive definite matrices efficiently.

ACKNOWLEDGMENTS

Aspects of the technology described in this paper are the subject of U.S. Provisional Patent Application No. 63/690,322, filed on September 4, 2024, and U.S. Provisional Patent Application No. 63/839,979, filed on July 8, 2025.

VII. REFERENCES SECTION

REFERENCES

- [1] G. H. Golub and C. F. Van Loan, *Matrix computations*. Johns Hopkins, 2013.
- [2] Y. Saad, *Iterative methods for sparse linear systems*. SIAM, 2003.
- [3] M. Horowitz, "1.1 computing's energy problem (and what we can do about it)," in *2014 IEEE International Solid-State Circuits Conference Digest of Technical Papers (ISSCC)*, 2014, pp. 10–14.
- [4] A. W. Harrow, A. Hassidim, and S. Lloyd, "Quantum algorithm for linear systems of equations," *Phys. Rev. Lett.*, vol. 103, p. 150502, Oct 2009. [Online]. Available: <https://link.aps.org/doi/10.1103/PhysRevLett.103.150502>
- [5] J. Preskill, "Quantum computing in the nisq era and beyond," *Quantum*, vol. 2, p. 79, 2018.
- [6] L. Gyongyosi and S. Imre, "A survey on quantum computing technology," *Computer Science Review*, vol. 31, pp. 51–71, 2019.
- [7] A. Sebastian, M. Le Gallo, R. Khaddam-Aljameh, and E. Eleftheriou, "Memory devices and applications for in-memory computing," *Nature nanotechnology*, vol. 15, no. 7, pp. 529–544, 2020.
- [8] D. Ielmini and H.-S. P. Wong, "In-memory computing with resistive switching devices," *Nature electronics*, vol. 1, no. 6, pp. 333–343, 2018.
- [9] D. B. Strukov, G. S. Snider, D. R. Stewart, and R. S. Williams, "The missing memristor found," *Nature*, vol. 453, no. 7191, pp. 80–83, 2008.
- [10] N. Taherinejad, P. S. Manoj, and A. Jantsch, "Memristors' potential for multi-bit storage and pattern learning," in *2015 IEEE European Modelling Symposium (EMS)*, 2015, pp. 450–455.
- [11] A. Irmanova and A. P. James, "Multi-level memristive memory with resistive networks," in *2017 IEEE Asia Pacific Conference on Postgraduate Research in Microelectronics and Electronics (PrimeAsia)*, 2017, pp. 69–72.
- [12] Z. Diao, R. Yamamoto, Z. Meng, T. Tohei, and A. Sakai, "Enhancing memristor multilevel resistance state with linearity potentiation via feedforward pulse scheme," *Nanoscale Horizons*, 2025.
- [13] M. Rao, H. Tang, J. Wu, W. Song, M. Zhang, W. Yin, Y. Zhuo, F. Kiani, B. Chen, X. Jiang *et al.*, "Thousands of conductance levels in memristors integrated on CMOS," *Nature*, vol. 615, no. 7954, pp. 823–829, 2023.
- [14] Z. Fahimi, M. R. Mahmoodi, M. Klachko, H. Nili, and D. B. Strukov, "The impact of device uniformity on functionality of analog passively-integrated memristive circuits," *IEEE Transactions on Circuits and Systems I: Regular Papers*, vol. 68, no. 10, pp. 4090–4101, 2021.
- [15] Y. Kim, T. Gokmen, H. Miyazoe, P. Solomon, S. Kim, A. Ray, J. Doevenspeck, R. S. Khan, V. Narayanan, and T. Ando, "Neural network learning using non-ideal resistive memory devices," *Frontiers in Nanotechnology*, vol. 4, p. 1008266, 2022.

- [16] A. Amirsoleimani, F. Alibert, V. Yon, J. Xu, M. R. Pазhouhandeh, S. Ecoffey, Y. Beilliard, R. Genov, and D. Drouin, "In-memory vector-matrix multiplication in monolithic complementary metal-oxide-semiconductor-memristor integrated circuits: design choices, challenges, and perspectives," *Advanced Intelligent Systems*, vol. 2, no. 11, p. 2000115, 2020.
- [17] M. R. Mahmoodi, A. F. Vincent, H. Nili, and D. B. Strukov, "Intrinsic bounds for computing precision in memristor-based vector-by-matrix multipliers," *IEEE Transactions on Nanotechnology*, vol. 19, pp. 429–435, 2020.
- [18] C. Bengel, J. Mohr, S. Wiefels, A. Singh, A. Gebregiorgis, R. Bishnoi, S. Hamdioui, R. Waser, D. Wouters, and S. Menzel, "Reliability aspects of binary vector-matrix-multiplications using reram devices," *Neuromorphic computing and engineering*, vol. 2, no. 3, p. 034001, 2022.
- [19] G. Choe, A. Lu, and S. Yu, "3d and-type ferroelectric transistors for compute-in-memory and the variability analysis," *IEEE Electron Device Letters*, vol. 43, no. 2, pp. 304–307, 2021.
- [20] W. Song, M. Rao, Y. Li, C. Li, Y. Zhuo, F. Cai, M. Wu, W. Yin, Z. Li, Q. Wei *et al.*, "Programming memristor arrays with arbitrarily high precision for analog computing," *Science*, vol. 383, no. 6685, pp. 903–910, 2024.
- [21] C. Li, M. Hu, Y. Li, H. Jiang, N. Ge, E. Montgomery, J. Zhang, W. Song, N. Dávila, C. E. Graves *et al.*, "Analogue signal and image processing with large memristor crossbars," *Nature electronics*, vol. 1, no. 1, pp. 52–59, 2018.
- [22] M. Hu, C. E. Graves, C. Li, Y. Li, N. Ge, E. Montgomery, N. Davila, H. Jiang, R. S. Williams, J. J. Yang *et al.*, "Memristor-based analog computation and neural network classification with a dot product engine," *Advanced Materials*, vol. 30, no. 9, p. 1705914, 2018.
- [23] Z. Sun and D. Ielmini, "Invited tutorial: Analog matrix computing with crosspoint resistive memory arrays," *IEEE Transactions on Circuits and Systems II: Express Briefs*, vol. 69, no. 7, pp. 3024–3029, 2022.
- [24] I. Richter, K. Pas, X. Guo, R. Patel, J. Liu, E. Ipek, and E. G. Friedman, "Memristive accelerator for extreme scale linear solvers," in *Government Microcircuit Applications & Critical Technology Conference (GOMACTech)*, 2015.
- [25] B. Feinberg, R. Wong, T. P. Xiao, C. H. Bennett, J. N. Rohan, E. G. Boman, M. J. Marinella, S. Agarwal, and E. Ipek, "An analog preconditioner for solving linear systems," in *2021 IEEE International Symposium on High-Performance Computer Architecture (HPCA)*, 2021, pp. 761–774.
- [26] M. Le Gallo, A. Sebastian, R. Mathis, M. Manica, H. Giefers, T. Tuma, C. Bekas, A. Curioni, and E. Eleftheriou, "Mixed-precision in-memory computing," *Nature Electronics*, vol. 1, no. 4, pp. 246–253, 2018.
- [27] B. Ulmann and D. Killat, "Solving systems of linear equations on analog computers," in *2019 Kleinheubach Conference*. IEEE, 2019, pp. 1–4.
- [28] Y. Huang, N. Guo, M. Seok, Y. Tsvividis, and S. Sethumadhavan, "Evaluation of an analog accelerator for linear algebra," *ACM SIGARCH Computer Architecture News*, vol. 44, no. 3, pp. 570–582, 2016.
- [29] J. Hasler and A. Natarajan, "Continuous-time, configurable analog linear system solutions with transconductance amplifiers," *IEEE Transactions on Circuits and Systems I: Regular Papers*, vol. 68, no. 2, pp. 765–775, 2020.
- [30] A. Natarajan and J. Hasler, "Analog solutions of systems of linear equations on a configurable platform," in *2020 IEEE International Symposium on Circuits and Systems (ISCAS)*. IEEE, 2020, pp. 1–5.
- [31] Z. Sun, G. Pedretti, E. Ambrosi, A. Bricalli, W. Wang, and D. Ielmini, "Solving matrix equations in one step with cross-point resistive arrays," *Proceedings of the National Academy of Sciences*, vol. 116, no. 10, pp. 4123–4128, 2019.
- [32] Z. Sun, G. Pedretti, D. Ielmini *et al.*, "Fast solution of linear systems with analog resistive switching memory (RRAM)," in *Proceedings of the 4th IEEE International Conference on Rebooting Computing, ICRC 2019*. Institute of Electrical and Electronics Engineers Inc., 2019, pp. 1–5.
- [33] P. Mannocci, G. Pedretti, E. Giannone, E. Melacarne, Z. Sun, and D. Ielmini, "A fully-analogue, universal primitive for linear algebra operations using resistive memories," *IEEE Trans. Circuits and Systems I: Regular Papers*, 2021.
- [34] K. D. Gremban, "Combinatorial preconditioners for sparse, symmetric, diagonally dominant linear systems," Ph.D. dissertation, School of Computer Science, Carnegie Mellon University, October 1996.
- [35] H. Fu, Q. Hong, C. Wang, J. Sun, and Y. Li, "Solving non-homogeneous linear ordinary differential equations using memristor-capacitor circuit," *IEEE Transactions on Circuits and Systems I: Regular Papers*, vol. 68, no. 11, pp. 4495–4507, 2021.
- [36] The MathWorks, Inc., *MATLAB R2022a*, MathWorks, Natick, MA, USA, 2022, <https://www.mathworks.com/products/matlab.html>.
- [37] Analog Devices, Inc., *LTspice XVII Version 17.1*, Analog Devices, Norwood, MA, USA, 2023, <https://www.analog.com/en/design-center/design-tools-and-calculators/ltspice-simulator.html>.
- [38] R. H. MacNeal, "Passive analog computers for structural analysis," *Journal of the Structural Division*, vol. 88, pp. 103–136, June 1962.
- [39] J. R. Silvester, "Determinants of block matrices," *The Mathematical Gazette*, vol. 84, no. 501, pp. 460–467, 2000. [Online]. Available: <http://www.jstor.org/stable/3620776>